



HAL
open science

MIMO Spectral Efficiency over Energy Consumption Requirements: Application to WSNs

Maha Ben Zid, Kosai Raouf, Ammar Bouallegue

► **To cite this version:**

Maha Ben Zid, Kosai Raouf, Ammar Bouallegue. MIMO Spectral Efficiency over Energy Consumption Requirements: Application to WSNs. International journal of communications, network and system sciences, 2012, 5 (2), pp.121-129. 10.4236/ijcns.2012.52016 . hal-00689922

HAL Id: hal-00689922

<https://hal.science/hal-00689922>

Submitted on 20 Apr 2012

HAL is a multi-disciplinary open access archive for the deposit and dissemination of scientific research documents, whether they are published or not. The documents may come from teaching and research institutions in France or abroad, or from public or private research centers.

L'archive ouverte pluridisciplinaire **HAL**, est destinée au dépôt et à la diffusion de documents scientifiques de niveau recherche, publiés ou non, émanant des établissements d'enseignement et de recherche français ou étrangers, des laboratoires publics ou privés.

MIMO Spectral Efficiency over Energy Consumption Requirements: Application to WSNs

Maha Ben Zid¹, Kosai Raouf², Ammar Bouallègue³

¹Departement Images et Signal (DIS), GIPSA-Lab, University of Grenoble, Grenoble, France

²Laboratory of Acoustics at University of Maine (LAUM), ENSIM, Le Mans, France

³TIC Department, 6^oCOM, National Engineering School of Tunis (ENIT), Tunis, Tunisia

Email: maha.ben-zid@gipsa-lab.grenoble-inp.fr, kosai.raouf@univ-lemans.fr, ammar.bouallegue@enit.rnu.tn

Received November 11, 2011; revised January 9, 2012; accepted January 20, 2012

ABSTRACT

This paper presents the evaluation of the “capacity to the total energy consumption per bit ratio” of multiple antennas systems with distributed fashion. We propose an adequate geometric channel modeling for the wireless communication system which operates in indoor propagation environment with scatterers. The channel model is derived in function of both the line of sight (LOS) and the non line of sight (NLOS) components. The aim of this paper is to study the limits in the gain concerning the capacity to the total energy consumption ratio when additional antennas are implemented in the communication system. To do so, we have evaluated by simulations both the capacity and the total energy consumption per bit. Then, we have determined the capacity to the total energy consumption ratio. Finally, the computational capacity to the total energy ratio is obtained for different system configurations. We have shown that the gain in capacity increases with the number of antennas but it stills be limited by the total energy consumption. The limits for increasing the number of transmit antennas are determined in function of the separation distances between the transmitter and the receiver sides of the communication system. Optimal power allocation strategy via water-filling algorithm has been carried out for evaluating the capacity to energy ratio. We find by simulation that optimal power allocation brings a gain in the addressed metric reaching a level of about 1.7 at transmit signal to noise ratio of 8 dB if comparing to the case when transmit energy is equally split among transmit antennas.

Keywords: MIMO Capacity; Energy Efficiency; Capacity to the Total Energy Consumption Ratio; Wireless Sensor Networks

1. Introduction

Multiple Input Multiple Output (MIMO) technology refers to the use of multiple antennas at the transmitter and/or multiple antennas at the receiver of the system communication. MIMO technology [1-4] has been shown to improve the communication system performance. It offers significant increases in spectral efficiency without additional bandwidth or transmit power. These features made MIMO technology attractive for several modern standards such as IEEE 802.11n, WiMax and 3GPP Long Term Evolution (LTE). We investigate the exploitation of MIMO systems in Wireless Sensor Networks (WSNs) where sensor nodes are miniature devices equipped with antennas. These nodes are randomly deployed in the sensing area and are assumed to operate until their batteries are exhausted. Therefore, energy management in such networks is a critical task. Throughout this paper, we show that even the use of multiple antennas system significantly improves the spectral efficiency of the communication system; it brings more requirements in terms

of the total energy consumption per bit. The behavior of the cost in terms of the total energy consumption as a function of the maximum achieved system capacity is presented in this paper. This will contribute to optimal design for the low-power high-efficiency communication system which corresponds to the number of antennas for which we can get the lowest costs in energy consumption for a required level of system capacity.

The contribution of this paper falls into the category of distributed algorithms. As our work focuses on the distributed environment, it is worthwhile to address the information collection problem in the design process. In literature, many algorithms may be implemented for decision-making information collection. Among the existing algorithms for the decision-making algorithms, we perform the Code Division Multiple Access (CDMA) acquisition technique [5,6]. The best choice of decision-making strategy is such that signal synchronization can be achieved in the minimum time. However, it should be noticed that unlike the performed methodology works

well, the performed algorithm presents a complexity during the synchronization process at the acquisition phase. In fact, the first step of processing at the receiver is to synchronize the generated pseudo-noise scrambling sequence to the tracking range of the received waveform. Nevertheless, the acquisition time is very long for long-duration pseudo-noise sequences since its mean acquisition time is proportional to the pseudo noise sequence period as several correlations need to be employed.

2. Paper Organization

The remainder of this paper proceeds as follows. Section 3 gives an overview of the multiple antennas systems and introduces to the application of MIMO technology in wireless sensor networks. Section 4 presents the channel model according to an indoor propagation environment with rich scatterers. The analysis of the capacity to energy ratio is detailed in Section 5. Simulation results are presented and analyzed in Section 6. The improvement in the capacity to energy ratio via water-filling is evaluated in Section 7. Finally, concluding remarks are summarized in Section 8.

3. Multiple Antennas System: Application to WSN

3.1. Multiple Antennas System: An Overview

We introduce in this section the communication system model for multiple antennas system. We assume that N_T antennas are deployed at the transmitter and N_R antennas are deployed at the receiver side as depicted in **Figure 1**. At the transmit side, each antenna T_{x_j} ;

$j=1, \dots, N_T$ sends the signal x_j ; $j=1, \dots, N_T$ to the receive antennas $R_{x_1}, \dots, R_{x_{N_R}}$. Signals x_j ;

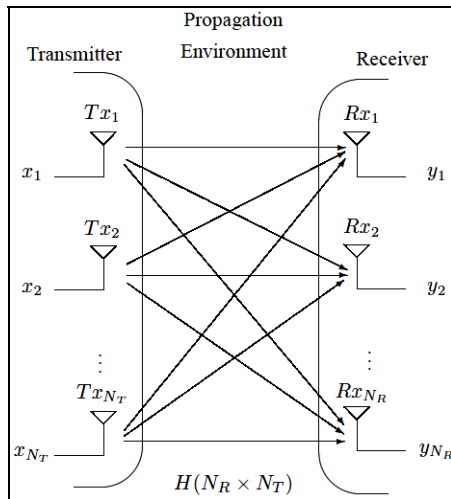


Figure 1. MIMO system model.

$j=1, \dots, N_T$ pass through the radio propagation channel.

The complex channel matrix $H(N_R \times N_T)$ is given by:

$$H = \begin{pmatrix} h_{11} & \cdots & h_{1N_T} \\ \vdots & \ddots & \vdots \\ h_{N_R1} & \cdots & h_{N_R N_T} \end{pmatrix}$$

h_{ij} , $j=1, \dots, N_T$; $i=1, \dots, N_R$ denotes the complex channel gain which links the transmit antenna T_{x_j} to the receive antenna R_{x_i} . At the receiver side, each receive antenna $R_{x_1}, \dots, R_{x_{N_R}}$ collects the incoming signals from the N_T transmit antennas which add up coherently. The received signals at antennas $R_{x_1}, \dots, R_{x_{N_R}}$ are respectively denoted in **Figure 1** by y_1, \dots, y_{N_R} . The received signal at antenna R_{x_i} ; $i=1, \dots, N_R$ with additive noise signal b_i ; $i=1, \dots, N_R$ is given by:

$$y_i = \sum_{j=1}^{N_T} h_{ij} x_j + b_i ; i=1, \dots, N_R \quad (1)$$

From matrix notations where:

- $x = [x_1, \dots, x_{N_T}]^T$ is the $(N_T \times 1)$ complex vector for the transmitted signal.
- $y = [y_1, \dots, y_{N_R}]^T$ is the $(N_R \times 1)$ complex vector for the received signal.
- $b = [b_1, \dots, b_{N_R}]^T$ is the $(N_R \times 1)$ complex vector for the additive noise signal.

The multiple antennas system model is described by the input output relationship as:

$$y = H \times x + b \quad (2)$$

3.2. MIMO Approach for WSNs

The work addressed in this paper is not limited to the MIMO systems. The structure of MIMO system is assumed to be performed by Wireless Sensor Networks (WSNs). The approach of MIMO systems is summarized in **Figure 2** where N_T sensor nodes S_{Tx_j} ; $j=1, \dots, N_T$,

are available at the transmit side and N_R sensor nodes S_{Rx_i} ; $i=1, \dots, N_R$ are considered at the receive side. Each sensor node S_{Tx_j} ; $j=1, \dots, N_T$ transmits its information x_j ; $j=1, \dots, N_T$ to all the other sensor nodes at the receiver side following the model described by Equation (2).

4. Channel Modeling

The Rician fading channel modeling is performed in this work. We assume that the channel coefficients vary in

function of the square value of the separation distance between the transmitter and the receiver. The channel matrix coefficients h_{ij} ; $j = 1, \dots, N_T$; $i = 1, \dots, N_R$ are given by:

$$h_{ij} = \frac{1}{\sqrt{1+K}} \cdot h_{ij}^{\text{NLOS}} + \sqrt{\frac{K}{1+K}} h_{ij}^{\text{LOS}} \quad (3)$$

K is the Rician coefficient.

The performed communication scenario assumes a rich scattering propagation environment with L_S scatterers as depicted in **Figure 3**.

The NLOS components are expressed as:

$$h_{ij}^{\text{NLOS}} = \frac{1}{\sqrt{L_S}} \sum_{l=1}^{L_S} \alpha_l \cdot \frac{1}{(d_{il} + d_{lj})^2} \quad (4)$$

- α_l is a random scattering coefficient from the l th scatterer, $l = 1, \dots, L_S$.
- d_{il} is the distance between the i th receive antenna and the l th scatterer, $i = 1, \dots, N_R$; $l = 1, \dots, L_S$.
- d_{lj} is the distance between the l th scatterer and the j th transmit antenna, $l = 1, \dots, L_S$; $j = 1, \dots, N_T$

The LOS components are given by:

$$h_{ij}^{\text{LOS}} = \frac{1}{(d_{ij})^2} \quad (5)$$

- d_{ij} is the distance between the i th receive antenna

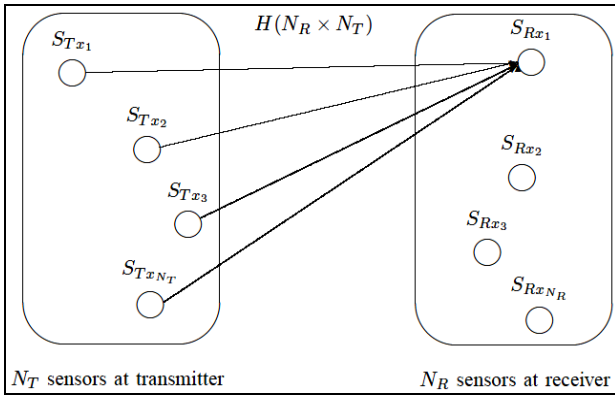


Figure 2. MIMO approach for WSNs.

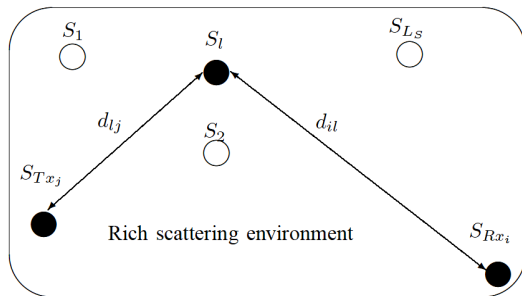


Figure 3. Propagation environment with scatterers.

and the j th transmit antenna, $i = 1, \dots, N_R$; $j = 1, \dots, N_T$.

5. Capacity to Energy Ratio Analysis

The metric R_0 [7] given by Equation (6) measures the capacity to the total energy consumption per bit ratio.

$$R_0 = \frac{\bar{C}}{E_{bt}} \quad (6)$$

- \bar{C} is the ergodic system capacity (in bits/s/Hz) given as the expectation value of the instantaneous channel capacity over channel matrices realizations.

$$\bar{C} = E_H(C) \quad (7)$$

- E_{bt} is the total energy consumption per bit (in J).

The computation of both the system capacity and the total energy consumption are detailed in the following sections.

5.1. Channel Capacity Evaluation

When no channel state information (CSI) is available at the transmitter, the transmit energy is equally split between the N_T antennas. As such, the instantaneous channel capacity [1] associated to the multiple antennas communication system model is given by:

$$C(H) = \log_2 \left[\det \left(I_{N_R} + \frac{\gamma_T}{N_T} \cdot HH^H \right) \right] \text{ bits/s/Hz} \quad (8)$$

γ_T denotes the transmit signal to noise ratio.

Case of available channel state information at both the transmitter and the receiver, the channel capacity may be computed in more optimal way by performing the water-filling algorithm [8]. The instantaneous channel capacity with water-filling is then:

$$C_{WF}(H) = \sum_{p=1}^R \log_2 \left[\left(\frac{\lambda_{H,p} \mu}{\sigma_n^2} \right)^+ \right] \text{ bits/s/Hz} \quad (9)$$

- R is the rank of the channel matrix H .
- σ_n^2 is the noise signal power.
- $a^+ = \max(a, 0)$.
- μ is a constant scalar that satisfies the total power constraint.
- $\lambda_{H,p}$ is the p th singular value of the channel matrix H .

In the following, we consider normalization for the channel matrix $H(N_R \times N_T)$ so that the power channel P_c satisfies:

$$P_c = N_T \times N_R$$

Where:

$$P_c = \|H\|_F^2 = E \left[\text{Tr}(H^H H) \right] = \sum_{i,j} P_{ij}; \quad P_{ij} = E \left[h_{ij}^2 \right] \quad (10)$$

- $\|H\|_F^2$ is the Frobenius norm.
- $Tr(\cdot)$ is the trace operator.

Based on the channel modeling that we have presented previously, we consider a MIMO system of dimensions $(N_R \times N_T)$ where the number of transmit antennas is variable and the number of receive antennas is fixed to 4. The simulation of system capacity is presented for different transmit signal to noise ratios γ_T of 2 dB, 4 dB and 8 dB. The separation distance between the transmitter and the receiver, d equals 20 meters. The variation of the system capacity as a function of the number of transmit antennas when performing water-filling is presented in **Figure 4**. The simulated ergodic capacity via water-filling algorithm is shown to be improved as well as more antennas are deployed at the transmitter and more energy is allocated.

5.2. Total Energy Consumption per Bit Evaluation

We evaluate the power consumption for each antenna at both the transmit and receive sides. For a given bit rate level, the energy consumption could be then deduced. Our analysis is based on the model of the transmitter block with complex modulator and the model of the receiver block as shown in **Figure 5** and **Figure 6**. These models are respectively performed by each transmit and receive antenna. The total power consumption [9,10] is evaluated in function of:

- 1) The power consumption of the amplifiers, P_{PA} .
- 2) The power consumption of the circuit blocks, P_C .

The power consumption of the amplifiers is expressed as:

$$P_{PA} = \frac{\xi}{\eta} P_{out} \quad (11)$$

- ξ is the peak to average ratio which is expressed as a

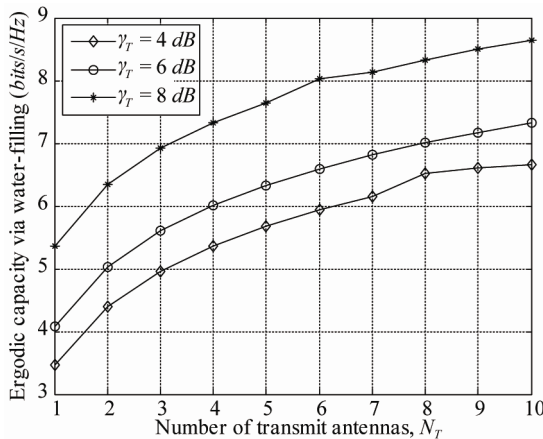


Figure 4. Multiple antennas system capacity with water-filling, $d = 20$ m.

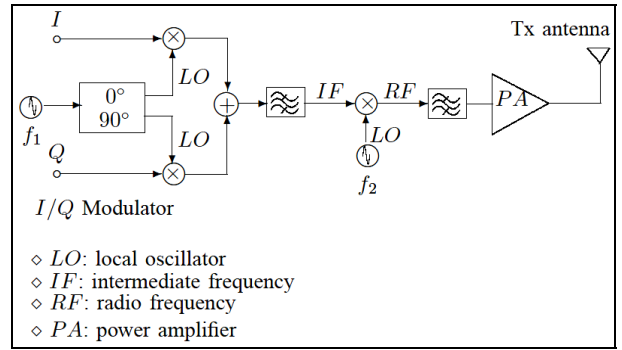


Figure 5. Transmit block diagram.

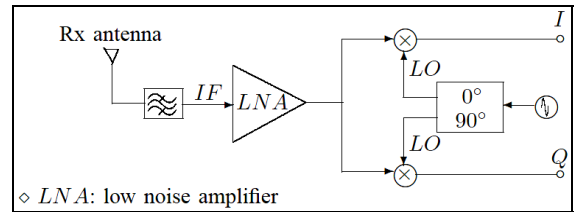


Figure 6. Receiver block diagram.

function of the modulation constellation size M by:

$$\xi = 3 \cdot \frac{M - 2\sqrt{M} + 1}{M - 1} \quad (12)$$

- η is the drain efficiency.

The output power for a separation distance between the transmitter and the receiver d is expressed as:

$$P_{out} = E_b \cdot R_b \cdot \frac{(4\pi)^2}{G_t G_r \lambda^2} \cdot d^\rho \cdot M_l \cdot N_f \quad (13)$$

E_b is the transmission energy per bit. For a required bit error rate, denoting the receive signal to noise ratio at each receive antenna by γ_R , when the transmit power is equally allocated to the N_T transmit antennas, the average error probability is:

$$\bar{P}_b = E_H \left[Q \left(\sqrt{2 \cdot \gamma_R} \right) \right] = E_H \left[Q \left(\sqrt{2 \cdot \|H\|_F^2 \cdot \frac{\gamma_T}{N_T}} \right) \right] \quad (14)$$

- $Q(\cdot)$ denotes the Marcum function.

An upper bound for the required energy per bit satisfies [9]:

$$\bar{P}_b \leq \left(\frac{\gamma_T}{N_T} \right)^{-N_T} \quad (15)$$

- R_b is the bit rate.
- G_t is the transmit antenna gain.
- G_r is the receive antenna gain.
- λ is the wavelength.
- ρ is the path loss exponent. The path loss exponent is assumed to be the same for all the propagation links.

For indoor propagation environment, the path loss exponent at a carrier frequency of 2.4 GHz equals 3.3 [11].

- M_l is the link margin.
- N_f is the receiver noise figure.

The total power consumption is evaluated by computing the power consumption of both the transmitter circuit blocks and the receiver circuit blocks of multiple antennas systems with N_T transmit antennas and N_R receive antennas as:

$$P_C \approx N_T \times (P_{MOD} + P_{DAC} + P_{mix} + P_{filt}) + \dots + 2 \times P_{syn} + \dots + N_R \times (P_{LNA} + P_{mix} + P_{IFA} + P_{fltr} + P_{ADC} + P_{DeMOD}) \quad (16)$$

- P_{MOD} : power consumption of the modulator.
- P_{DAC} : power consumption of the digital-to-analog converter.
- P_{mix} : power consumption of the mixer.
- P_{filt} : power consumption of the active filter at the transmitter.
- P_{syn} : power consumption of the frequency synthesizer.
- P_{LNA} : power consumption of the low-noise amplifier.
- P_{IFA} : power consumption of the intermediate frequency amplifier.
- P_{fltr} : power consumption of the active filter at the receiver.
- P_{ADC} : power consumption of the analog-to-digital converter.
- P_{DeMOD} : power consumption of the demodulator.

Finally, we express the total energy consumption per bit as:

$$E_{bt} = \frac{(P_{PA} + P_C)}{R_b} \quad (17)$$

6. Simulation Results and Observations

In order to evaluate the metric ‘‘capacity to energy ratio’’, we have carried out a computer based Monte-Carlo simulation for both the distributed MIMO system capacity and the total energy consumption per bit following the communication system model as introduced in Section 3.1. **Table 1** summarizes the system setting. The number of receiver antennas N_R is set to 4. The metric ‘‘capacity to energy ratio’’ is evaluated for different transmitter configurations with variable number of transmit antennas N_T .

6.1. Energy Simulation

We investigate the analysis of the effect of separation distance between the transmitter and the receiver on the ‘‘capacity to energy ratio’’ for each transmitter antennas

configuration. The total energy consumption per bit is simulated for separation distances between the transmitter and the receiver in the range from 1 m to 20 m.

Figure 7 shows the plotted curves of the total energy consumption as a function of the number of transmit antennas for different separation distances between the transmitter and the receiver. The total energy consumption per bit is shown to increase as well as more antennas are deployed at the transmitter. We report in **Table 2**, the growth in energy consumption when comparing to the total energy consumption of MMO (4×1). The transmit signal to noise ratio is $\gamma_T = 8$ dB and the separation distance between the transmitter and the receiver is set to

Table 1. Simulation parameters.

Simulation parameter	Value
Constellation size, M	2
Separation distance, $d(m)$	[1,20]
Noise power	-120 dBm
Carrier frequency	2.4 GHz
Bandwidth	2.4 MHz
Bit rate, R_b	10 kbit/s
Antenna gain product	$G_t \cdot G_r = 5$ dB
Drain efficiency, η	0.35
Link margin, M_l	40 dB
Receiver noise figure, N_f	10 dB
Noise power spectral density	-174 dBm/Hz
Number of scatterers, L_s	30
Path loss exponent, ρ	3.3
P_{MOD}	30 mW
P_{DeMOD}	30 mW
P_{DAC}	40 mW
P_{ADC}	40 mW
P_{mix}	30.3 mW
P_{filt}	2.5 mW
P_{fltr}	2.5 mW
P_{syn}	50 mW
P_{LNA}	20 mW
P_{IFA}	3 mW

Table 2. Growth in the total energy consumption per bit with various number of antennas.

N_T	2	4	6	8
$\frac{E_{bt}(N_T)}{E_{bt}(N_T=1)}$	1.13	1.38	1.89	1.98

$d = 10$ m. The impact of the separation distance on energy consumption is evaluated in **Table 3**. Here, we are evaluating the growth in energy consumption when comparing the separation distance between the transmitter and the receiver of 10 m and 20 m.

In the following, we propose to examine the behavior of the total energy consumption per bit for different constellation sizes at fixed transmit signal to noise ratio of 8 dB and number of transmit antennas $N_T = 4$. The total energy consumption per bit is presented in **Figure 8** as a function of the separation distance between the transmitter and the receiver d for various modulation constella-

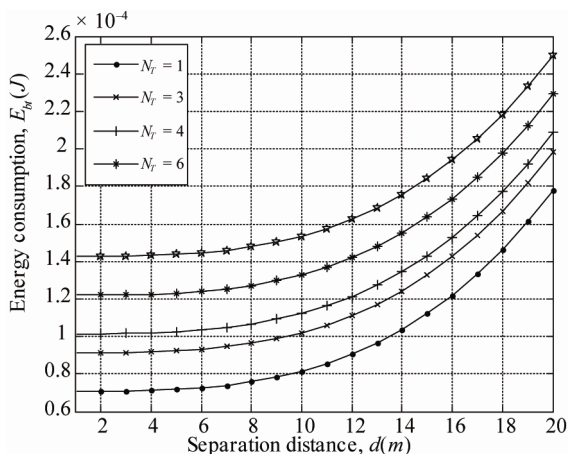


Figure 7. Total energy consumption per bit over separation distance and variable number of transmit antennas.

Table 3. Growth in the total energy consumption per bit with various separation distances.

N_T	2	4	6	8
$\frac{E_b(d=20\text{ m})}{E_b(d=10\text{ m})}$	2.06	1.86	1.73	1.63

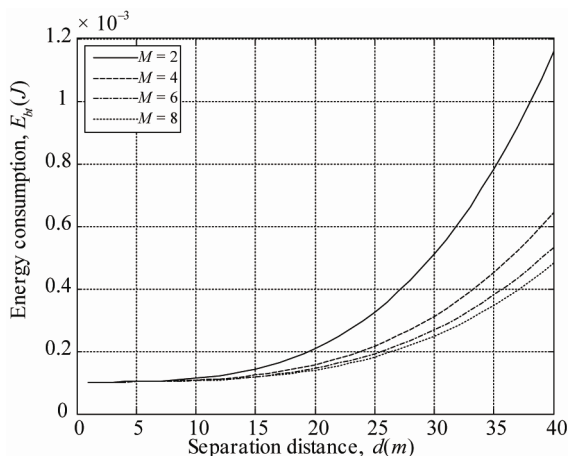


Figure 8. Energy consumption for various constellation sizes, M .

tion sizes $M = 2, M = 4, M = 6$ and $M = 8$. The presented results show that higher modulation constellation size permits saves in the total energy consumption. The gain in the total energy consumption is more important for higher separation distances between the transmitter and the receiver.

Table 4 evaluates the saving in the total energy consumption in function of the constellation size expressed as:

$$Gain_M = 1 - \left(\frac{E_{bt}(M)}{E_{bt}(M=2)} \right) \tag{18}$$

As we have shown by simulation in Section 5.1 that the use of multiple antennas considerably improves the communication system capacity as well as how the use of multiple antennas could be costly in the total energy consumption per bit in Section 6.1, we propose in the following to evaluate the limits in the use of additional antennas that still improve the capacity to energy ratio, R_0 .

6.2. Capacity to Energy Ratio Simulation

The metric “capacity to energy ratio” represents the amount of energy required for a given system capacity. The simulation of the metric R_0 is targeted to examine how much the use of additional antennas could improve the metric “capacity to energy ratio”. The simulation results of the metric R_0 are sketched in **Figure 9**. We assume that the transmit energy is equally split between the N_T antennas. **Figure 10** shows that the metric R_0 decreases in function of the separation distance between the transmitter and the receiver.

The behavior of the capacity to energy ratio over distance d is expected since the capacity decreases in function of the separation distance and the total energy consumption per bit is increased. We also find by simulation that R_0 decreases in function of the number of antennas N_T as sketched in **Figure 11**.

6.3. Capacity to Energy Ratio: Water-Filling

We investigate in this section, the use of water-filling algorithm on the simulation of the capacity to energy ratio, R_0 . **Figure 12** shows the variation of the capacity to energy ratio for different separation distances. We

Table 4. Impact of the constellation size on the total energy consumption per bit.

	$Gain_4$	$Gain_6$	$Gain_8$
$d = 10$ m	4%	6%	7%
$d = 20$ m	25%	30%	33%
$d = 40$ m	44%	54%	59%

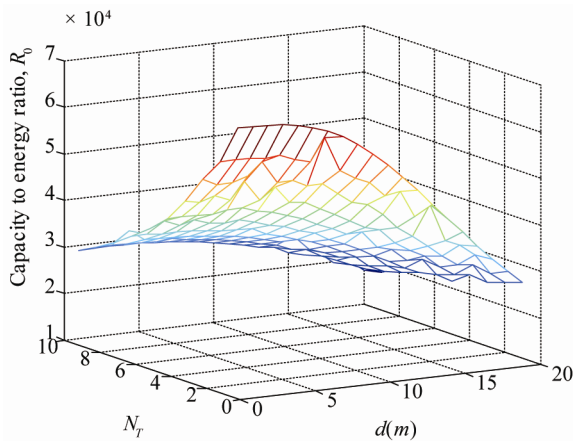


Figure 9. Capacity to energy ratio over the number of transmit antennas and separation distances, $M = 2$.

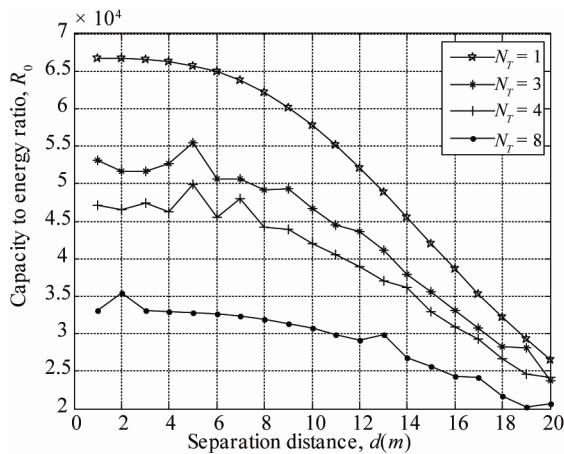


Figure 10. Capacity to energy ratio for various separation distances.

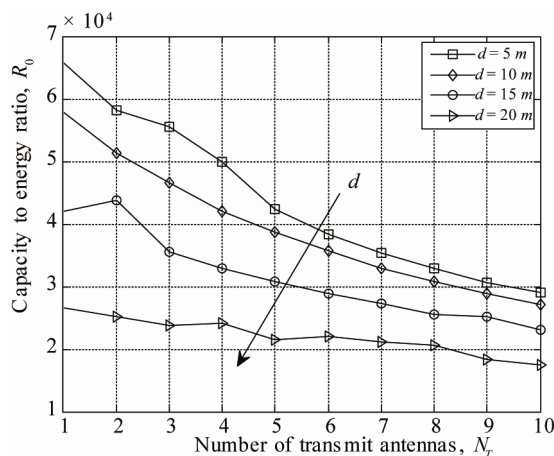


Figure 11. Capacity to energy ratio for various number of transmit antennas.

keep our comments as previously concerning the behavior of R_0 which decreases in function of the separation

distance between the transmitter and the receiver, d . The variation of R_0 in function of the antenna number is sketched in **Figure 13** ($\gamma_T = 8 \text{ dB}$) and **Figure 14** ($\gamma_T = 3 \text{ dB}$).

The capacity to energy ratio grows with the number of transmit antennas but it is shown to be limited by the number of receive antennas $N_R = 4$. All possible variations of the capacity to energy ratio at $\gamma_T = 3 \text{ dB}$ are reported in **Figure 15**.

7. Improvement in the Capacity to Energy Ratio via Water-Filling

We evaluate in this section, via a comparative analysis the ratio between the metric obtained via water-filling and that one when no water-filling is performed. γ_T is set to 8 dB and M equals 2. **Figure 16** depicts the gain in the metric R_0 when power is optimally allocated among the transmit antennas. The improvement in the capacity to energy ratio R_0 is presented for different separation

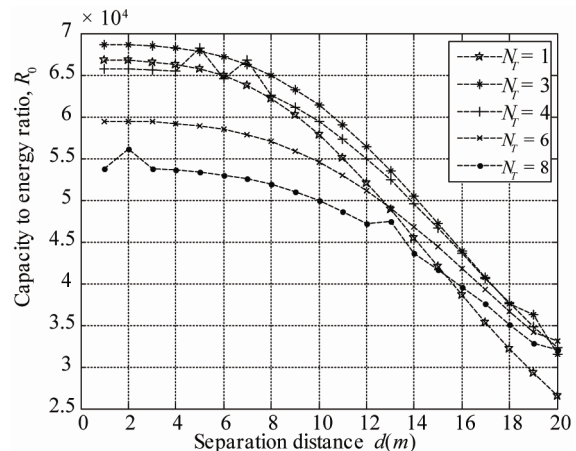


Figure 12. Capacity to energy ratio over separation distance (water-filling).

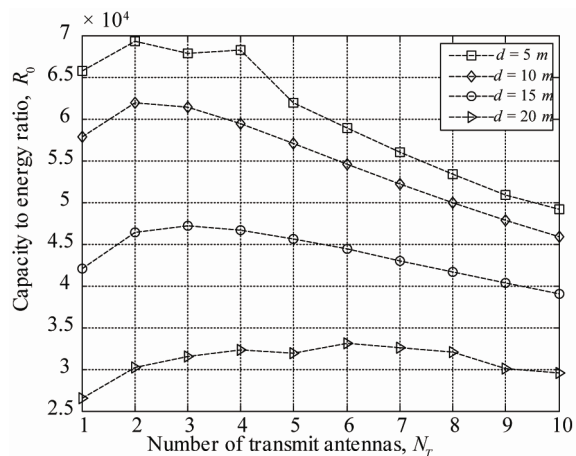


Figure 13. Capacity to energy ratio over the number of transmit antennas (water-filling), $\gamma_T = 8 \text{ dB}$.

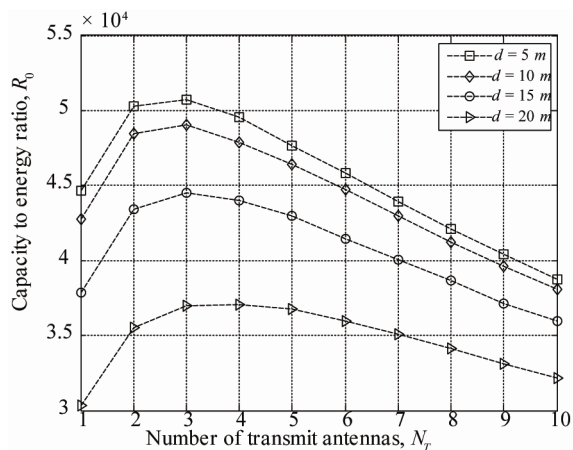


Figure 14. Capacity to energy ratio over the number of transmit antennas (water-filling), $\gamma_T = 3\text{ dB}$.

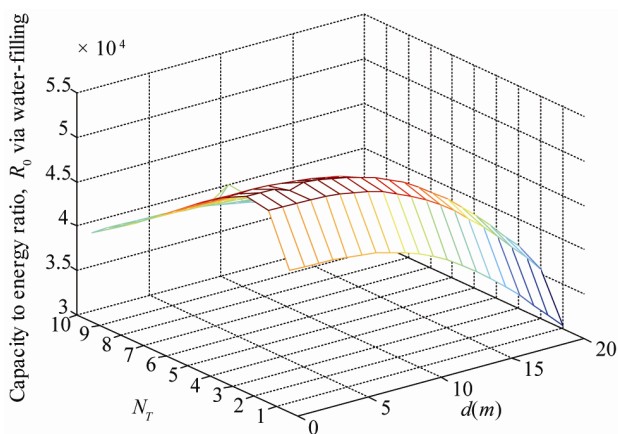


Figure 15. Simulated capacity to energy ratio via water-filling, $\gamma_T = 3\text{ dB}$.

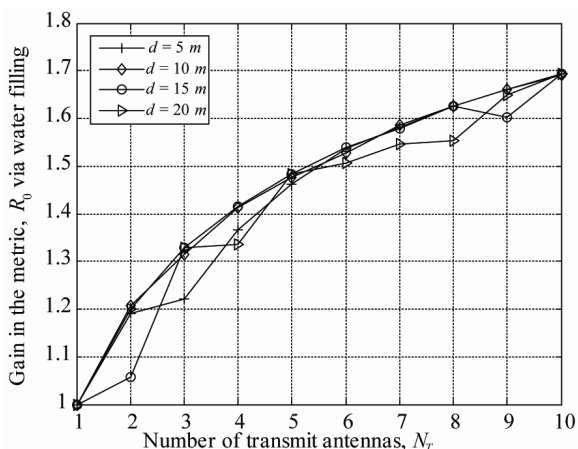


Figure 16. Improvement in the capacity to energy ratio via water-filling.

distances between the transmitter and the receiver but seems to be insensible to the separation distance between the transmitter and the receiver. The improvement in the

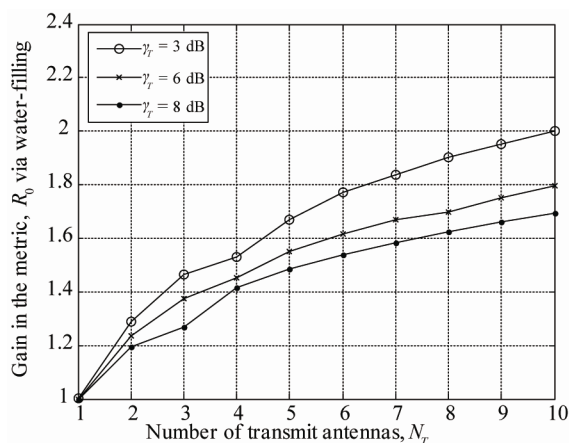


Figure 17. Improvement in the capacity to energy ratio via water-filling for different SNRs, γ_T .

capacity to the total energy ratio is presented at separation distance of 10 m in Figure 17 when different levels of the transmit signal to noise ratio, γ_T are considered. As depicted in Figure 17, the gain in the metric R_0 is more important for the lowest transmit signal to noise ratio γ_T .

8. Conclusion

Throughout this paper, we have made the analysis of the capacity to the total energy consumption per bit for multiple antennas systems with fixed number of receive antennas and various number of transmit antennas. To do so, the metric R_0 has been introduced in order to evaluate the cost in energy consumption for a given amount of the communication system capacity. Our analysis has been carried out over the Rician channel model with scatterers. Simulation of the capacity to energy ratio has been presented for variable number of transmit antennas and different ranges of the separation distances between the transmitter and the receiver. We have presented our results when optimal transmit power allocation is exploited and we have shown that even the use of multiple antennas improves the system capacity, it stills be limited by the total energy consumption. The IEEE 802.15.4 standard and ZigBee wireless technology could be considered for the evaluation of the presented communication model and could be then tested easily via a simple method of data routing.

REFERENCES

- [1] K. Raouf, M. Ben Zid, N. Prayongpun and A. Bouallègue, "Advanced MIMO Techniques: Polarization Diversity and Antenna Selection," 2011. <http://www.intechopen.com>
- [2] K. Raouf and H. Zhou, "Advanced MIMO Systems," Scientific Research Publishing, USA, 2009.

- [3] M. Ben Zid, K. Raoof and A. Bouallègue, "MIMO Systems and Cooperative Networks Performances," In: K. Raoof, *et al.*, *Cognitive Radio*, Scientific Research Publishing, USA, 2011, pp. 113-140.
- [4] E. Biglieri, R. Calderbank, A. Constantinides, A. Goldsmith and A. Paulraj, "MIMO Wireless Communications," Cambridge University Press, Cambridge, 2007.
- [5] B. Lang, T. Han and X. Gu, "A Robust Non-Coherent Sequential Code Acquisition Scheme for DS/SS Communications," *Proceedings of the 9th International Conference on Signal Processing (ICSP'08)*, Beijing, 26-29 October 2008, pp. 1939-1942.
- [6] G. S. Hosangadi and C. W. Baum, "Hybrid Sequential Acquisition Schemes for Noncoherent Chip-Asynchronous DS/SS Systems," *Proceedings of the IEEE International Conference on Communications (ICC'98)*, Atlanta, 7-11 June 1998, pp. 1242-1247.
- [7] M. Ben Zid, K. Raoof and A. Bouallègue, "A Novel Metric for Measuring Multiple Antennas System Capacity over Energy Consumption Requirements," *Proceedings of the 7th International Conference Wireless Communications, Networking and Mobile Computing (WiCOM)*, Wuhan, 23-25 September 2011, pp. 1-4.
- [8] M. A. Khalighi, J.-M. Brossier, G. V. Jourdain and K. Raoof, "Waterfilling Capacity of Rayleigh MIMO Channels," *Proceedings of the 12th IEEE International Symposium on Personal, Indoor and Mobile Radio Communications*, San Diego, 30 September-3 October 2001, pp. 155-158.
- [9] S. Cui, A. J. Goldsmith and A. Bahai, "Energy-Efficiency of MIMO and Cooperative MIMO Techniques in Sensor Networks," *IEEE Journal on Selected Areas in Communications*, Vol. 22, No. 6, 2004, pp. 1089-1098. [doi:10.1109/JSAC.2004.830916](https://doi.org/10.1109/JSAC.2004.830916).
- [10] S. Cui, A. J. Goldsmith, and A. Bahai, "Energy-constrained modulation optimization," *IEEE Transactions on Communications*, Vol. 4, No. 5, 2005, pp. 2349-2360.
- [11] K. Kaemarungsi and P. Krishnamurthy, "Modeling of Indoor Positioning Systems Based on Location Fingerprinting," *Proceedings of the 23rd Annual Joint Conference of the IEEE Computer and Communications Societies*, Hong Kong, March 2004, pp. 1012-1022.